Photon-number correlations near the threshold of microcavity lasers in the weak-coupling regime

R. Jin, D. Boggavarapu, M. Sargent III, P. Meystre, H. M. Gibbs, and G. Khitrova
Optical Sciences Center, University of Arizona, Tucson, Arizona 85721
(Received 13 December 1993)

The quantum-noise properties near the threshold of microcavity lasers are studied theoretically and experimentally in the weak-coupling regime. Computations based on two-level quantum theory show that the microlasers exhibit a high degree of second-order coherence compared with conventional lasers as a result of the suppression of spontaneous emission into nonlasing modes, and that there always exists a finite threshold for these lasers defined by the peak of the photon-number correlation function corresponding to the spontaneous-to-stimulated transition.

PACS number(s): 42.50.−p, 42.55.−f

The study of radiative properties of atoms in tailored electromagnetic environments, cavity quantum electrodynamics (QED), is a topic of considerable interest [1]. Most such studies originated in the microwave regime, where it is relatively easy to build closed, single-mode resonators and to completely turn off spontaneous emission. In contrast, optical experiments invariably involve open resonators, and spontaneous emission into free space always contributes to mask true cavity QED effects.

Generically, it is possible to classify cavity QED experiments with the help of three rates, which are traditionally called γ', κ, and g in the quantum optics literature: γ' gives the spontaneous emission rate into free-space modes in the presence of a cavity, and is related to the cavityless free-space spontaneous emission rate γ by a geometrical factor which depends on the solid angle sustained by the resonator; κ measures the resonator losses; and g is a measure of the (dipole) coupling between the atoms and the cavity mode. Two main regimes of cavity QED can then be identified: in the weak-coupling regime, g is smaller than one of the decay rates κ and γ', where γ' can be significantly different from γ; and in the strong-coupling regime, g is the dominant rate. (In contrast, conventional quantum optics and laser physics are characterized by the inequality $g<\gamma',\kappa$.) The strong-coupling regime has been the subject of considerable studies in the microwave regime, and in particular, the micromaser [2] operates in the regime $g\gg\kappa,\gamma'\approx 0$. Recently, it has also become possible to reach the strong-coupling regime at optical frequencies [3,4], and evidence of the strong atom-field coupling, e.g., in the form of "reversible" spontaneous emission and of a significant vacuum Rabi splitting has been found experimentally.

The weak-coupling regime, which is still characterized by irreversible spontaneous emission, but possibly enhanced [5] or inhibited [6], is also of considerable interest. For instance, it has been suggested that a laser operating in this regime would become "thresholdless" in the limit when $\gamma'\rightarrow 0$ [7]. This has led to considerable activities toward developing appropriate cavities in the optical frequency region, through the use of multilayer structures [8], high quality modes and mirrors [9], or "photonic bandgap" structures [10].

In this paper, we outline the theory of a laser operating in the weak-coupling cavity QED regime and compare it with experiments. Of particular interest here is a discussion of the "threshold" of such a laser. Historically, the laser threshold has been theoretically described in terms of an analogy between the laser and a nonequilibrium phase transition [11]. In the thermodynamic limit, it is characterized as a second-order-like phase transition, the derivative of the output intensity as a function of the pump parameter exhibiting a discontinuity at threshold. This transition is accompanied by large intensity fluctuations that can be observed in the second-order intensity correlations function [12]. As γ' decreases and a larger fraction of photons emits into the lasing mode, one reaches the cavity QED regime of microcavity lasers, where the concept of a phase transition, strictly speaking, loses its meaning and, hence, what is meant by a threshold becomes somewhat unclear. In particular, the derivative of the intensity ceases to be discontinuous and to be a useful way to describe the threshold because as $\gamma'\rightarrow 0$ all emission (whether spontaneous or stimulated) must go into the lasing mode. On the other hand, we show that the intensity fluctuations of the field still exhibit a maximum because of the transition from spontaneous to stimulated emission. This leads us to propose that the point at which this maximum is reached should be used as the definition of the threshold for microcavity lasers.

The quantum theory of a microlaser operating in the weak-coupling cavity QED regime is straightforward in principle. The active medium is coupled to two baths, one which describes spontaneous emission into the free-space modes and gives rise to the decay rate γ', and the other which describes the damping of the cavity mode at rate κ [13]. In addition, the active medium is coupled to the field mode with the coupling constant g. Since we are in the weak-coupling regime, all standard approximations of laser theory can still be carried through, and the only effective changes are in the various decay rates entering the equations. The photon statistics are derived via a quantum theory based on the density-matrix equations of

motion [14–17]. Two remarks need to be made at this point. First, the transverse relaxation rate $1/T_2$ of the atomic transition depends in general both on elastic collisions and on spontaneous emission, and hence is changed from its free-space value in cavity QED situations. However, if the laser medium is collision dominated, such as in semiconductor lasers, we can neglect the effects of spontaneous emission and use the free-space value of this rate. Second, the rate γ' is quite complicated to compute from first principles for a given cavity geometry, and is treated here as a phenomenological factor [18].

In this paper, we consider specifically the case of a two-level laser with upper-level to ground-level-lower-level decay [17]. This configuration describes the three-level pumping scheme appropriate for the ruby laser as well as some aspects of the semiconductor laser, for which the pump occurs directly from the valence band to the conduction band. We assume that the upper laser transition is pumped at rate Λ from the lower state (e.g., through a fast decaying third level) and that both thermal baths are at zero temperature, an excellent approximation in the optical regime. The photon-number probability p_n is then readily found to be

$$\frac{dp_n}{dt} = -(n+1)A_{n+1}p_n + (n+1)B_{n+1}p_{n+1} + nA_np_{n-1} - nB_np_n \ , \tag{1}$$

where n is the photon number and $A_n = N_aR/2T_1(1+nR)$, $B_n = N_bR/2T_1(1+nR)$. $N_a = N'\Lambda T_1$, and $N_b = N'\gamma' T_1$ are the normalized zero-field populations of the upper and lower laser levels, with $T_1 = (\Lambda+\gamma')^{-1}$, $R = 4g^2T_1T_2$ ($g^2 = \pi^2\wp^2\mathcal{E}_\omega^2/2h^2$, where $\wp$, $\mathcal{E}_\omega$, and h are the dipole matrix element, the electric field per photon, and the Planck's constant, respectively), and N' being the total number of atoms contributing to lasing. The microlasers are usually characterized in terms of a phenomenological "spontaneous emission factor" β [18], which is defined as the ratio of emission into the laser mode to the total emission, and is related to parameters in our theory by $\beta \approx (1+\gamma'/2g^2T_2)^{-1}$. In our model, the effect of suppressed spontaneous emission in microlasers is a reduction of the "pumping" $N'\gamma'$ of the lower-state population, which, in turn, reduces the absorption term B_n. Hence the emission term A_n does not have to compensate for as much absorption as in the case of conventional lasers, thus resulting in a reduction of the laser threshold. In steady state, the master equation (1) yields the photon statistics

$$p_n = p_0 \prod_{k=1}^{k=n} \frac{N_a}{N_b + 2T_1(R^{-1}+k)\kappa} \ , \tag{2}$$

where p_0 is the probability of no photon, and acts as a normalization constant. We concentrate here on the second moment of the photon statistics, and specifically compute the Fano-Mandel parameter [1,19] $K = [\langle n^2\rangle - \langle n\rangle^2 - \langle n\rangle]/\langle n\rangle = \langle n\rangle[g^{(2)}(0)-1]$ for various values of β and κ. These results are then compared with measurements carried out with a GaAs microcavity laser operating in a range where our simple two-level laser theory can give reasonable results. Note that although semiconductor lasers cannot in general be described by this simple theory, we expect it to describe the tuning-independent features of bulk semiconductor lasers corresponding to those given by the widely used linear density gain model [20], as long as appropriate effective medium parameters are used. We shall see that, indeed, our theory does yield reasonable qualitative agreement with the experiment.

The experimental setup (see Fig. 1) is a standard Hanbury-Brown–Twiss [21] arrangement previously used by Armstrong and Smith [12] to measure photon bunching near the threshold of a conventional GaAs laser. The top and bottom mirrors of the microcavity laser studied in our experiment consist of 22 and 27.5 periods of 62.5-nm AlGaAs (Al concentration = 0.143)/73.3-nm AlAs quarter-wave stacks with designed reflectivities exceeding 0.999 near the lasing wavelength (the actual reflectivities are around 0.998 [22]). The active region has 0.7357 μm of bulk GaAs. The entire laser structure is grown on a semi-insulating GaAs substrate by molecular beam epitaxy. Unlike conventional lasers with many closely spaced cavity modes inside the gain bandwidth [12,23], the short cavity length of the microcavity laser ensures that there is only one longitudinal cavity mode in the entire gain and high-reflectivity frequency band. The pump source is a SDL diode laser with stabilized current (110 mA) and temperature (14.9 °C) control. The 830-nm pump beam is focused to a spot with a 5-μm effective diameter on the microcavity laser (which is kept at room

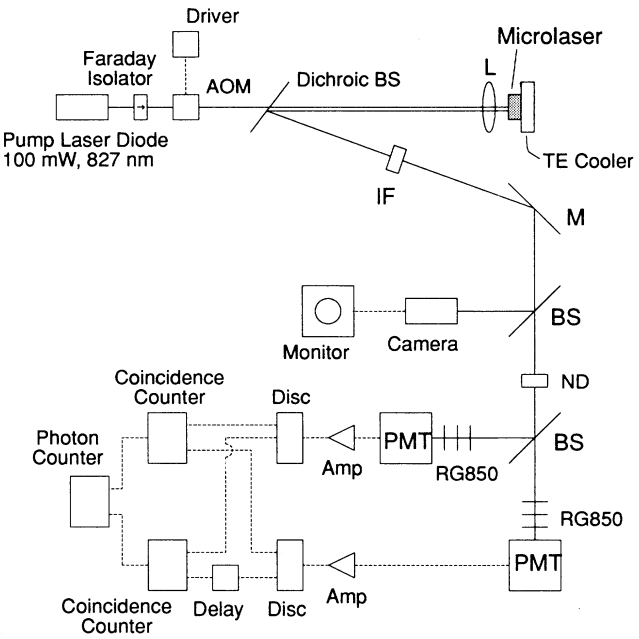

FIG. 1. Experimental setup for measurement of photon correlations. The symbols used in the figure are AOM—acousto-optic modulator, IF—interference filter, BS—beam splitter, L—lens, TE cooler—thermoelectric cooler, M—mirror, ND—neutral density filter, RG850—edge filter that transmits wavelengths longer than 850 nm, PMT—photomultiplier tubes, Amp—amplifiers, and Disc—discriminators.

temperature) by an antireflection coated diode laser lens after passing through an acousto-optic modulator and a Faraday isolator. The acousto-optic modulator is used to adjust the pump level, and the Faraday isolator prevents any feedback into the pump laser. The resulting pump power fluctuations are measured by a precision digital power meter to be less than 10^{-4}. A dichroic beam splitter sends the output of the microcavity laser to a 50%-50% beam splitter, which divides the beam into two beams of equal intensity before sending them to two photomultiplier tubes (the bias voltage is adjusted to achieve an optimum signal-to-noise ratio). The photogenerated electric pulses from each channel pass through two stages of amplification before they are directed to an EGG Ortec Model 583 differential discriminator. Each discriminator has two output channels. The first output channels are connected using 50-Ω impedence BNC cables to one coincidence counter. The second output channels, with a long (>150 ns) delay between them, are connected to a second coincidence counter to measure random coincidences. The output of each coincidence circuit is sent to the input of a SRS Model SR400 counter unit. The single-channel count rate is kept at 10^6 counts/s via a variable neutral density filter, and the time resolution of the entire coincidence circuitry is about 3.5 ns. Data are

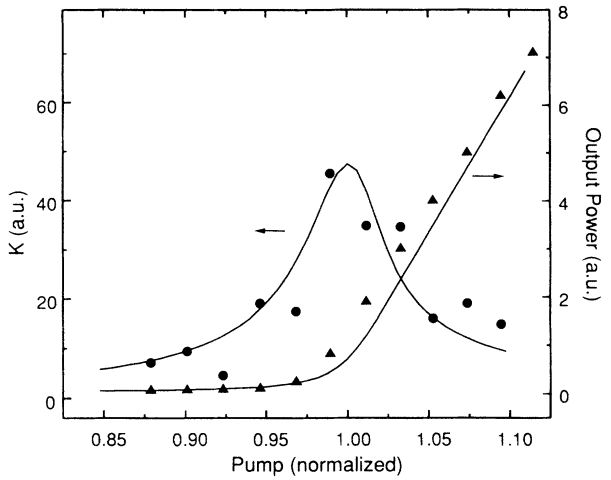

FIG. 2. The measured output power (triangles) and photon-number fluctuations (circles) of a GaAs microcavity laser. The pump power is normalized such that $\Lambda=1$ corresponds to the peak in the K curve, which is used to define Λ_{th} (Λ_{th} in the experimental curve is about 6.8 mW). The solid lines are theoretical plots. The parameters used in the computation are $Q=2000$ and $\gamma'=0.8$ GHz, which correspond to the experimental conditions.

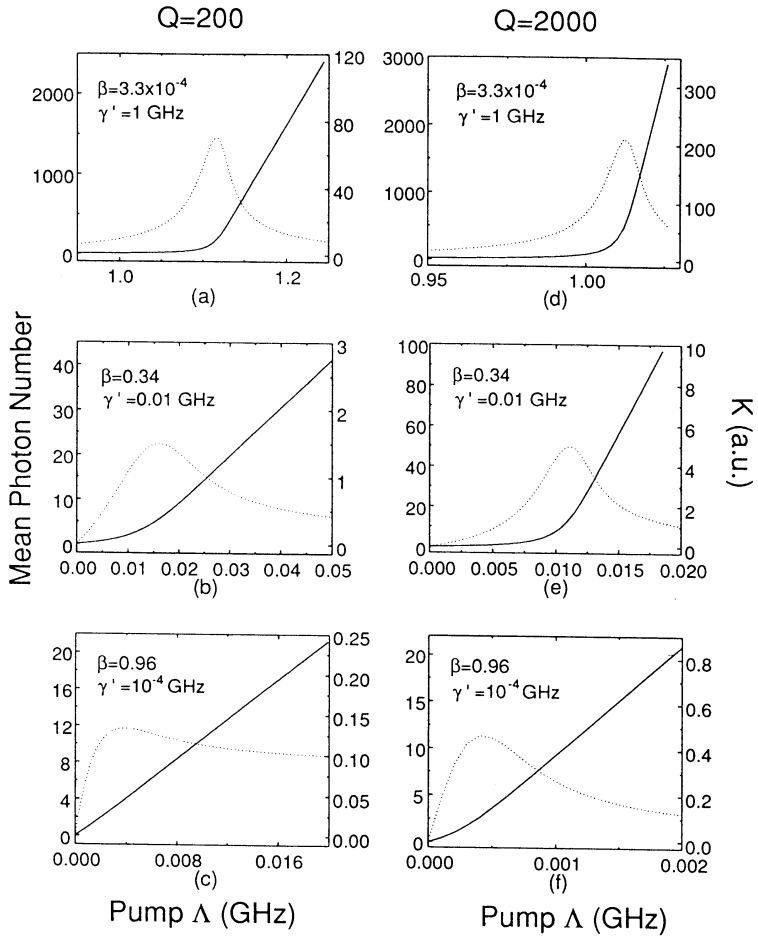

FIG. 3. The theoretical average photon number (solid lines) and the correlation function K (dotted lines) for various β and Q. Different horizontal and vertical scales are used for clarity. (a) and (d) correspond to the case of a conventional laser with small β, while others describe microlasers with larger β. (a)–(c) are for $Q=200$, and (d)–(f) are for $Q=2000$.

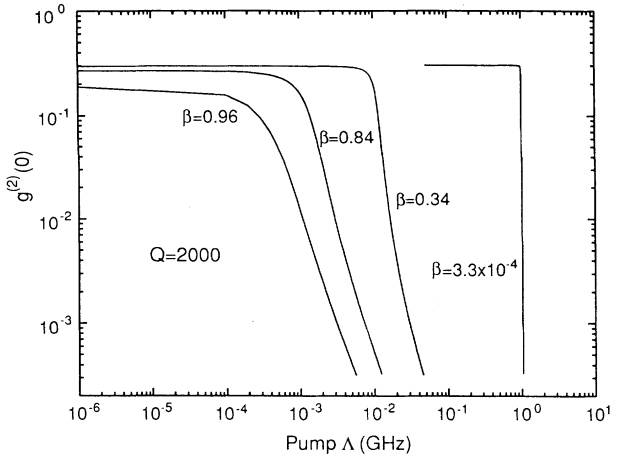

FIG. 4. The second-order coherence function $g^{(2)}(0)$ as a function of pump for various β.

taken for 5 min at each pump level, where both the random and the correlated coincidence counts are recorded. The measured photon-number correlations as a function of the pump power are shown in Fig. 2. The derivative-of-intensity threshold and the peak-of-K threshold agree very well for the microcavity used in the experiment with $\beta=6.5\times10^{-3}$ ($\gamma'=0.8$ GHz). This value is more than an order of magnitude larger than those of typical conventional lasers [12,23], but still not large enough to illustrate the derivative-of-intensity thresholdlessness.

To compute the photon statistics, we use the effective experimental values appropriate for the GaAs microcavity laser used in our experiment: they are $N'=2.5\times10^{7}$, $T_2=10^{-13}$ s, and $g=3.7\times10^{9}$ s^{-1} ($\wp=4.8\times10^{-29}$ m C, $V=25$ μm^3). Furthermore, we express the cavity damping rate κ in terms of its quality factor Q via $\kappa=\omega/Q$, where ω is the angular frequency of the laser transition. From the measured Fabry-Pérot étalon full width at half maximum (FWHM) of 1.7 Å, we deduce an effective mirror reflectivity of $R_{\text{eff}}=0.993$. Since the optical field extends well into the Bragg reflectors, the effective cavity length is estimated from multilayer calculations of our microlaser structure to be about 2.2 μm. Thus we obtain $Q\approx2000$ for the lasing mode given by $Q=\omega L/c\ln(1/R_{\text{eff}})$ [16]. Figure 2 shows good agreement between our experimental results and the steady-state results of Eq. (2).

Whereas we have not yet fabricated a microcavity with a large β, our model, which is certainly valid for any value of β, enables us to reach important conclusions on the statistical properties of so-called thresholdless lasers. The theoretical curves of Fig. 3 allow us to compare the derivative-of-intensity threshold with the peak-of-K threshold for very large β. The main result is that the former disappears whereas the Fano-Mandel parameter still clearly exhibits a peak indicative of enhanced intensity fluctuations near threshold. For instance, while the growth in intensity as a function of the pump parameter almost follows a straight line in Figs. 3(c) and 3(f), $K(\Lambda)$ still exhibits a well-defined peak. We argue that this peak should be used as a proper definition of the threshold of a weak-coupling microlaser. Based on this definition, the microlaser never becomes strictly thresholdless; the quality of the emitted light below the peak-K threshold does not possess the degree of coherence usually associated with laser emission even though the derivative of intensity would make it appear thresholdless.

Another interesting outcome of our study is summarized in Fig. 4, which shows the normalized second-order correlation function $g^{(2)}(0)=\langle I^2(0)\rangle/\langle I(0)\rangle^2$ of the microlaser as a function of the β factor. These results show that as β is increased, $g^{(2)}(0)$ at very low pumping is already less than the thermal source value of 2 and closer to 1, characteristic of Poissonian photon statistics of a coherent state [24]. This is mainly due to the cutback of the number of nonlasing modes which are largely responsible for the intensity noise. Hence, microlasers operating in the weak-coupling regime have reduced (although still classical) intensity fluctuations compared to a standard laser operating at the same pump power. On the other hand, it has recently been shown that they also exhibit a larger linewidth [25]. We are, then, led to the conclusion that although microlasers are difficult to distinguish from light-emitting diodes (LED's) from their spectral characteristics, their higher-order correlation functions, which demonstrate a high degree of second-order coherence, are fundamentally different. It should be noted that the reduced value of $g^{(2)}(0)$ below threshold, however, is still much larger than that of a highly coherent light source, such as in the case of a conventional laser above threshold. Thus the determination of the threshold of microcavity lasers by the peak of the Fano-Mandel parameter is of great importance in practical situations that require a high degree of second-order coherence.

In summary, we have outlined the quantum theory of a weak-coupling microlaser and compared it with experiments. We found good agreement between the predicted and measured values of the second-order correlation of the field for low β. The theoretical results for high β values stress the importance of using the peak in the Fano-Mandel parameter of the field as a definition of the microlaser threshold. There is no thresholdless laser if second-order coherence (laser intensity noise) is the criterion. We have also shown that while the spectral properties of these lasers, which resemble those of LED's, make them of questionable use in interferometric-type applications, they exhibit a strong degree of second-order coherence as a function of the pump rate, and might be of considerable interest in amplitude-modulation-type applications.

We thank S. W. Koch for helpful discussions, and S. Jacobs and T. Milster for the pump-laser diode setup. We also thank the JSOP (AFOSR and ARO), NSF-LWT, OCC, DARPA, and ONR for their support of this work.

[1] For recent reviews, see P. Meystre, in *Progress in Optics,* edited by E. Wolf (Elsevier, New York, 1992) Vol. XXX; S. Haroche, in *Fundamental Systems in Quantum Optics,* edited by J. Dalibard, J. M. Raimond, and J. Zinn-Justin (North-Holland, Amsterdam, 1992).
[2] D. Meschede, H. Walther, and G. Muller, Phys. Rev. Lett. **54**, 551 (1985).
[3] See, e.g., M. G. Raizen, R. J. Thompson, R. J. Brecha, H. J. Kimble, and H. J. Carmichael, Phys. Rev. Lett. **63**, 240 (1989).
[4] C. Weisbush, M. Nishioka, A. Ishikawa, and Y. Arakawa, Phys. Rev. Lett. **69**, 3314 (1992).
[5] E. M. Purcell, Phys. Rev. **69**, 681 (1946).
[6] D. Kleppner, Phys. Rev. Lett. **47**, 233 (1981).
[7] F. De Martini and G. R. Jacobovitz, Phys. Rev. Lett. **60**, 1711 (1988).
[8] J. L. Jewell, K. F. Huang, K. Tai, Y. H. Lee, R. J. Fischer, S. L. McCall, and A. Y. Cho, Appl. Phys. Lett. **55**, 424 (1989).
[9] S. L. McCall, A. F. Levi, R. E. Slusher, S. J. Pearton, and R. A. Logan, Appl. Phys. Lett. **60**, 289 (1992); R. E. Slusher, Opt. Phot. News **4**, 8 (1993); A. F. J. Levi, R. E. Slusher, S. L. McCall, J. L. Glass, S. J. Pearton, and R. A. Logan, Appl. Phys. Lett. **62**, 561 (1993).
[10] E. Yablonovitch, Phys. Rev. Lett. **58**, 2059 (1987).
[11] V. de Giorgio and M. O. Scully, Phys. Rev. A **2**, 1170 (1970); R. Graham and H. Haken, Z. Phys. **237**, 31 (1970).
[12] A. W. Armstrong and J. A. Smith, Phys. Rev. Lett. **14**, 68 (1965); J. A. Smith and A. W. Armstrong, *ibid.* **16**, 1169 (1966).
[13] H. J. Carmichael, R. J. Brecha, M. G. Raizen, M. Xiao, and H. J. Kimble, J. Opt. Soc. Am. B **3**, 238 (1986); C. M. Savage, Quantum Opt. **2**, 89 (1990).
[14] M. O. Scully and W. E. Lamb, Jr., Phys. Rev. **159**, 208 (1967).
[15] M. Sargent, III, M. O. Scully, and W. E. Lamb, Jr., Appl. Opt. **9**, 2423 (1970).
[16] M. Sargent III, M. O. Scully, and W. E. Lamb, *Laser Physics* (Addison-Wesley, Reading, MA, 1977).
[17] P. Meystre and M. Sargent III, *Elements of Quantum Optics,* 2nd ed. (Springer-Verlag, Berlin, 1991).
[18] Y. Suematsu, S. Akiba, and T. Hong, IEEE J. Quantum Electron. **QE-13**, 596 (1977); T. Bada *et al.*, *ibid.* **27**, 1347 (1991).
[19] L. Mandel, Opt. Commun. **42**, 356 (1982).
[20] A. Yariv, *Quantum Electronics,* 3rd ed. (Wiley, New York, 1989).
[21] R. Hanbury-Brown and B. Q. Twiss, Nature (London) **177**, 27 (1956); **178**, 1046 (1956).
[22] R. Jin, D. Boggavarapu, G. Khitrova, H. M. Gibbs, Y. Z. Hu, S. W. Koch, and N. Peyghambarian, Appl. Phys. Lett. **61**, 1883 (1992).
[23] F. T. Arecchi, G. S. Rodari, and A. Sona, Phys. Lett. **25A**, 59 (1967).
[24] R. J. Glauber, Phys. Rev. Lett. **10**, 84 (1963).
[25] S. W. Koch, Bull. Am. Phys. Soc. **38**, 98 (1993).

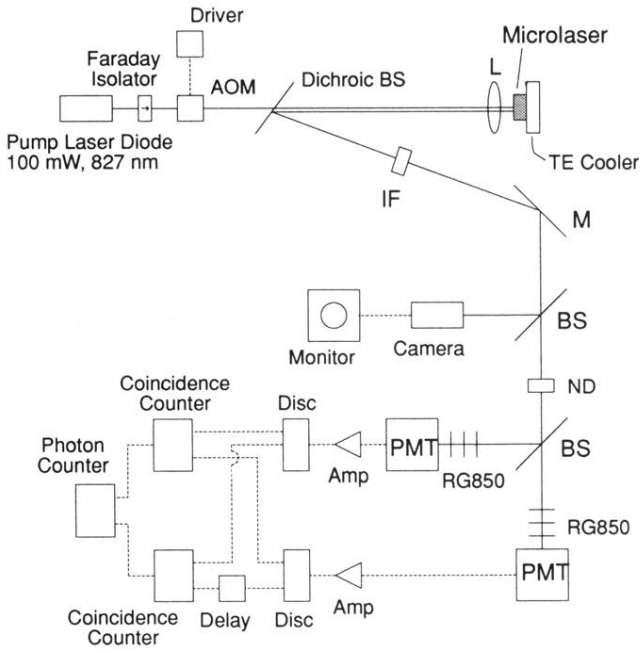

FIG. 1. Experimental setup for measurement of photon correlations. The symbols used in the figure are AOM—acousto-optic modulator, IF—interference filter, BS—beam splitter, *L*—lens, TE cooler—thermoelectric cooler, *M*—mirror, ND—neutral density filter, RG850—edge filter that transmits wavelengths longer than 850 nm, PMT—photomultiplier tubes, Amp—amplifiers, and Disc—discriminators.